

# A Dynamic Model of the Disk Drive Spindle Motor and Its Applications

W. N. Fu, Z. J. Liu, and C. Bi

**Abstract**—A dynamic model of the hard disk-drive spindle motor based on the circuit-field-motion coupled-time-stepping finite-element method is presented. The model provides a basis for determining back electromotive force, inductance, and cogging torque in dynamic operation conditions. The merits of the proposed method are that the estimation of the motor parameters can be obtained, accounting for the saturation effect and other operational conditions, and the computing time for parameters calculation can be reduced. The proposed model can also be used to determine the commutation time, cogging torque, output torque, and radial force, to study the effect of the skewed magnets/slots, and to simulate the starting process and other transient processes.

**Index Terms**—Finite element, motors, parameter computation.

## I. INTRODUCTION

SPINDLE motor is a key component in the hard disk drives of modern computers. Its performance directly determines the capacity and quality of the disk drives [1]. It is expected that the spindle motor has enough starting torque, limited starting current, small torque ripple, and balanced radial magnetic force. The magnetic field computation using finite-element method (FEM) is now an indispensable tool in the analysis and design of the motor [2]. However, FEM-based modeling for system-level simulation of the spindle motor performance that results from coupled physical processes involving control electronics (circuit), electromagnetic field (field), and system kinetics (motion) remains a technical challenge to design engineers and researchers.

In this paper, a time-stepping FEM model of the spindle motor is presented. The FEM equations are directly coupled with the circuit equations of the armature windings and the motion equation. The model is useful for simulation of transient processes, and for accurate prediction of the lumped parameters of the spindle motor. The techniques to determine the commutation time, the estimation of the back electromotive force (e.m.f.), the cogging torque, and the inductance when the motor is in dynamic operation condition are also presented. The advantages of the proposed parameter estimation methods are that the saturation of iron materials can be directly included and the computing time can be reduced.

Manuscript received July 5, 2001; revised October 25, 2001.

W. N. Fu was with the Data Storage Institute, National University of Singapore, Singapore 117608. He is now with Ansoft Corporation, Pittsburgh, PA 15219 USA (e-mail: wfu@ansoft.com).

Z. J. Liu and C. Bi are with Data Storage Institute, National University of Singapore, Singapore 117608 (e-mail: dsiliuzj@dsi.nus.edu.sg).

Publisher Item Identifier S 0018-9464(02)02756-5.

## II. FEM METHOD OF THE SPINDLE MOTOR

### A. Basic Equations

A multislice two-dimensional (2-D) FEM is used for modeling the motor performance to account for the effect of skewed magnets or slots [3]. Maxwell's equations, applied to the domains, will give rise to the diffusion equations

$$\left. \begin{aligned} \nabla \times (\nu \nabla \times \mathbf{A}) &= 0, & \text{in irons and air gap} \\ \nabla \times (\nu \nabla \times \mathbf{A}) - \frac{i_s}{S} &= 0, & \text{in armature windings} \\ \nabla \times (\nu_{\text{PM}} \nabla \times \mathbf{A}) &= \nabla \times (\nu_{\text{PM}} \mathbf{B}_r), & \text{in permanent magnets} \end{aligned} \right\} \quad (1)$$

where

$\mathbf{A}$  magnetic vector potential (having the component of axial direction only, in this equation);

$\nu$  reluctivity of the material;

$i_s$  armature phase current;

$S$  total cross-sectional area of one turn on one coil side (parallel branches are considered as one turn);

$\mathbf{B}_r$  remanent flux density of the PM;

$\nu_{\text{PM}}$  equivalent reluctivity.

The field equations of all slices are connected by the circuit equations. The armature circuit equation of one phase is

$$\left[ N_{\phi 1} \sum_{m=1}^M l_m \left( \iint_{\Omega_m^+} \frac{\partial A}{\partial t} d\Omega - \iint_{\Omega_m^-} \frac{\partial A}{\partial t} d\Omega \right) \right] / \times \sum_{m=1}^M \iint_{\Omega_m^+ + \Omega_m^-} d\Omega + R_1 i_s + L_\sigma \frac{di_s}{dt} = v_s \quad (2)$$

where

$R_1$  total armature resistance of one phase winding;

$L_\sigma$  inductance of the end windings;

$N_{\phi 1}$  total number of the serial connected conductors per phase;

$v_s$  phase voltage on the winding;

$\Omega^+$ ,  $\Omega^-$  cross-sectional areas of the "in" and "out" side of the phase conductors of the coils, respectively.

The motor is divided into  $M$  slices and  $l_m$  is the axial length of the  $m$ th slice.

The mechanical movement equation is

$$T_e = T_L + J_M \frac{d\omega_r}{dt} + D\omega_r \quad (3)$$

$T_L$  load torque;

$J_M$  mechanical inertia of the rotor;

$D\omega_r$  damping torque;

$D$  damping coefficient which describes the rate of energy dissipation due to windage and frictional losses;

$T_e$  developed electromagnetic torque of the machine.

The electromagnetic torque can be computed using Maxwell stress tensor method [4]. The Maxwell tensor can be expressed as

$$\sigma = \frac{1}{\mu_0}(\mathbf{B} \cdot \mathbf{n})\mathbf{B} - \frac{1}{2\mu_0}(B^2\mathbf{n})\mathbf{B}. \quad (4)$$

Because

$$\mathbf{B} = B_r\mathbf{e}_r + B_\theta\mathbf{e}_\theta \quad B = \sqrt{B_r^2 + B_\theta^2} \quad (5)$$

one then has

$$\sigma = \frac{1}{2\mu_0}(B_r^2 - B_\theta^2)\mathbf{e}_r + \frac{1}{\mu_0}(B_r B_\theta)\mathbf{e}_\theta. \quad (6)$$

It can also be expressed as

$$\sigma = \frac{1}{2\mu_0} \{ [(B_r^2 - B_\theta^2) \cos \theta - 2B_r B_\theta \sin \theta] \mathbf{e}_x + [(B_r^2 - B_\theta^2) \sin \theta + 2B_r B_\theta \cos \theta] \mathbf{e}_y \}. \quad (7)$$

A closed integration circular path that surrounds the rotor in free space along the air-gap is chosen. The force in the tangential component is

$$\begin{aligned} F_\theta &= \frac{1}{r_s - r_r} \int_{r_r}^{r_s} \sum_{m=1}^M l_m \int_0^{2\pi} \left( \frac{1}{\mu_0} B_r B_\theta \right) r d\theta dr \\ &= \frac{1}{\mu_0(r_s - r_r)} \sum_{m=1}^M l_m \iint_{S_{ag}} B_r B_\theta dS \end{aligned} \quad (8)$$

where

- $r_s, r_r$  outer and inner radii of the circular ring, respectively;
- $S_{ag}$  cross-sectional area of the path;
- $r$  radius varying between the inner and outer radii of the path;
- $B_r, B_\theta$   $r$ - and  $\theta$ -components of the flux density, respectively;

Hence, the output torque  $T_e$  can be obtained by integration along the circular path

$$T_e = \frac{1}{\mu_0(r_s - r_r)} \sum_{m=1}^M l_m \iint_{S_{ag}} r B_r B_\theta dS. \quad (9)$$

Similarly, according to (7), the components of the radial magnetic force in the  $x$  and  $y$  directions can be calculated by

$$\begin{aligned} F_x &= \frac{1}{2\mu_0(r_s - r_r)} \sum_{m=1}^M l_m \\ &\times \iint_{S_{ag}} [(B_r^2 - B_\theta^2) \cos \theta - 2B_r B_\theta \sin \theta] dS \end{aligned} \quad (10)$$

$$\begin{aligned} F_y &= \frac{1}{2\mu_0(r_s - r_r)} \sum_{m=1}^M l_m \\ &\times \iint_{S_{ag}} [(B_r^2 - B_\theta^2) \sin \theta + 2B_r B_\theta \cos \theta] dS. \end{aligned} \quad (11)$$

When the windings are star-connected with an isolated center point, additional external circuit equations are required [5]. The inputs are the line voltages, and the phase voltages are also unknowns in the system equations. The input voltages are determined according to the control algorithms and the feedbacks of the phase currents, phase voltages, speed, and rotor position. The FEM equations together with the armature circuit equations, the torque balance equation, and the external circuit equations of the armature windings will give rise to the large non-linear equations of the system. The Backward Euler's method is used to discretize the time variable.

### B. Determination of the Commutation Time

In the spindle motor, the line voltages of the armature windings of each phase are controlled by power electronic switching elements such as MOSFET. The commutation time must be carefully chosen in order to maximize the output torque of the motor. Because the complicated relationship between the distribution of the armature windings and the magnetic poles, it is better if the commutation time is automatically determined by computation.

There are two methods to determine the commutation time. One method is based on e.m.f. waveform. The e.m.f. is computed when the armature currents equal zero and the rotor rotates at a constant speed. The commutation time is determined by the principle that the maximum e.m.f. should be obtained when its associated winding is conducted. Another method is based on torque waveform. The output torque is computed when the two phase windings have constant currents and the rotor rotates at a constant speed. The commutation time is determined by the principle that during the state of two-phase-on which lasts for  $60^\circ$  electrical degree, the average torque should reach the maximum. The computation shows that the two methods can give very close results.

### C. Estimation of the E.M.F., the Cogging Torque, and the Inductance in Dynamic Operations

The cogging torque and the inductance of the armature windings can be computed according to the magnetic field computations when there are no armature currents and no magnetic excitation, respectively. However, this method cannot include the effect of the saturation of iron materials. The proposed method is that these computations should be done synchronously with the time stepping computation of the simulation of the on-load operation. At each time step, when the magnetic field computation of the on-load operation is completed, the reluctivities of each element are fixed and the currents in the armature windings are set to zero, the magnetic field is computed again. The torque obtained by this method is the cogging torque but including the saturation of iron cores.

For the computation of the inductance, no other field computation is required because

$$\begin{aligned} v_s &= R_1 i_s + e = R_1 i_s + \frac{d}{dt}(\psi) = R_1 i_s + \frac{d}{dt}(L i_s) + e_0 \\ &= R_1 i_s + \frac{d}{dt}(L i_s + \psi_0) \end{aligned} \quad (12)$$

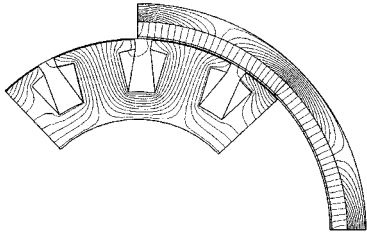


Fig. 1. Cross-section and computed flux plot of 8p12s spindle motor.

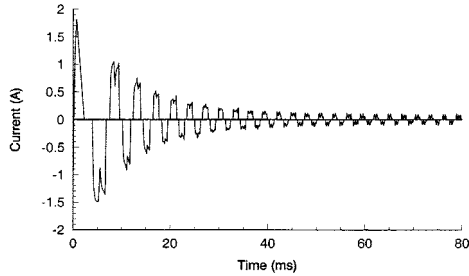


Fig. 2. Computed phase current during the starting process (8p12s).

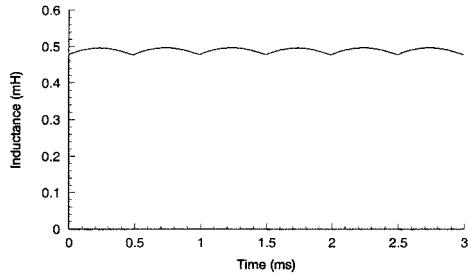


Fig. 3. Computed inductance on-load operation (8p12s).

where

$e, \psi$  e.m.f. and flux-linkage computed when the motor is in on-load operation, respectively;

$e_0, \psi_0$  e.m.f. and flux-linkage computed when the armature currents are set to zero, respectively;

$L$  inductance of the armature.

The inductance at the  $k$ th step can be obtained by

$$L^k = \frac{\psi^k - \psi_0^k}{i_s^k}. \quad (13)$$

Using this method, only one additional magnetic field computation is required. The incremental method can be used for this linear problem when the ICCG method is used for the solution; then the computing time can be greatly reduced [6].

### III. EXAMPLES

#### A. A Spindle With 8 Poles and 12 Slots (8p12s)

A three phase-winding spindle motor (12 V, 8 poles, 12 stator slots, star-connected, 5000 rpm) using Nd-Fe-B magnet for the field excitation, as shown in Fig. 1, is used to demonstrate the proposed method. The motor is driven by a converter with two-phase-on excitation. In the multislice FEM, the motor is divided into six slices, and at each slice, the mesh has 4201 nodes with 7386 elements. The length of the time step is 7.14  $\mu$ s. The computed phase current during the starting process are shown

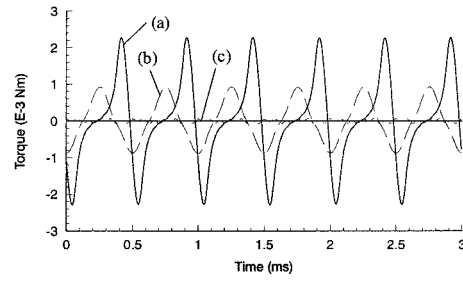


Fig. 4. Computed cogging torque (8p12s). (a) Magnets are not skewed. (b) Magnets are skewed 0.25 of one stator slot pitch. (c) Magnets are skewed 0.5 of one stator slot pitch.

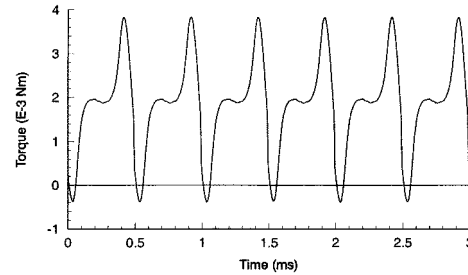


Fig. 5. Computed torque in on-load operation (magnets are not skewed, 8p12s).

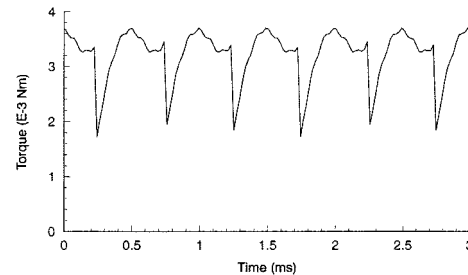


Fig. 6. Computed torque in on-load operation (magnets are skewed 0.5 of one stator slot pitch, 8p12s).

TABLE I  
COMPARISON OF COMPUTED COGGING TORQUE WHEN CHOOSING DIFFERENT SKEWED MAGNETS (SLICE NUMBER = 6)

Skewed stator slot pitch	$T_{\max}$ (m Nm)	$ T_{\text{av}} $ (m Nm)
0.00	2.283	0.873
0.25	0.927	0.496
0.50	0.068	0.033
0.75	0.413	0.173
1.00	0.454	0.266

in Fig. 2. The waveform of the inductance during on-load operation is shown in Fig. 3. The cogging torque and output torque when the magnets are nonskewed and skewed are shown in Figs. 4–6, and also compared in Tables I and II ( $T_{\text{MD}}$  is the mean value of the torque ripple). The magnetic force in radial direction is equal to zero because it counterbalances each other.

#### B. A Spindle With 8 Poles and 9 Slots (8p9s)

To compare the performance between 8p9s and 8p12s, the design parameters of an 8-pole 9-slot motor are kept the same as the 8p12s motor studied earlier, except that the width of slots

TABLE II  
COMPARISON OF COMPUTED TORQUE IN ON-LOAD OPERATION WHEN CHOOSING DIFFERENT SKEWED MAGNETS (SLICE NUMBER = 6)

Skewed stator slot pitch	$T_{av}/I_{rms}$ (m Nm/A)	$T_{MD}/I_{rms}$ (m Nm/A)
0.00	15.34	6.167
0.25	15.17	2.768
0.50	14.62	1.595
0.75	13.34	1.723
1.00	12.10	1.956

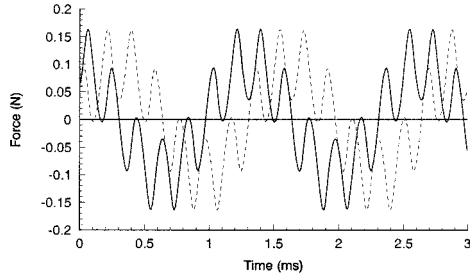


Fig. 7. Unbalanced force  $F_x$  and  $F_y$  in no load current condition (magnets are not skewed, 8p9s).

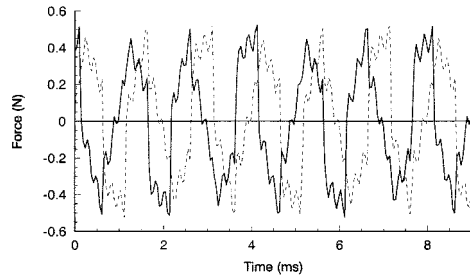


Fig. 8. Unbalanced force  $F_x$  and  $F_y$  in on-load operation (magnets are not skewed, 8p9s).

TABLE III  
PERFORMANCE COMPARISON BETWEEN 8p12s AND 8p9s (NONSKEWED)

	8p12s	8p9s
Cogging torque $T_{max}$ (m Nm)	2.283	0.295
$ T _{av}$ (m Nm)	0.873	0.129
Torque constant when on-load $T_{av}/I_{rms}$ (m Nm/A)	15.34	16.27
Torque ripple when on-load $T_{MD}/I_{rms}$ (m Nm/A)	6.167	1.972
Radial force when no current $ F _{av}$ (N)	0.0	0.1092
Radial force when on-load $ F _{av}$ (N)	0.0	0.4287

is increased 12/9 time. The waveforms of the computed unbalanced force are shown in Figs. 7 and 8. The performance comparisons between 8p12s motor and 8p9s motor when the PM is nonskewed and skewed are listed in Table III and IV.

TABLE IV  
PERFORMANCE COMPARISON BETWEEN 8p12s AND 8p9s (SKEWED)

	8p12s	8p9s
Skewed stator slot pitch	0.5	0.125
Cogging torque $T_{max}$ (m Nm)	0.068	0.000025
$ T _{av}$ (m Nm)	0.033	0.000009
Torque constant when on-load $T_{av}/I_{rms}$ (m Nm/A)	14.62	16.23
Torque ripple when on-load $T_{MD}/I_{rms}$ (m Nm/A)	1.595	1.919
Radial force when no current $ F _{av}$ (N)	0.0	0.09568
Radial force when on-load $ F _{av}$ (N)	0.0	0.4340

#### IV. CONCLUSION

The proposed 2-D multislice FEM is a powerful modeling tool for analyzing the performance of spindle motors. During the time-stepping computation, the motor parameters can also be computed then the effect of the saturation of the iron materials and other operational conditions can be precisely included in the solution. From the computed results, the following conclusions can be obtained: 1) 8p12s motor and 8p9s motor have very similar values of the output to volume ratio; 2) 8p12s motor has large cogging torque. 8p9s motor has small cogging torque; 3) 8p12s motor has no unbalanced radial force. 8p9s motor has large unbalanced radial force; 4) in on-load operation the radial force is more than doubled than that under zero armature current condition; and 5) the skewed PM can reduce the cogging torque of the 8p12s motor but cannot significantly reduce the cogging torque of the 8p9s motor.

#### REFERENCES

- [1] M. A. Jabbar, "Disk drive spindle motors and their controls," *IEEE Trans. Ind. Electron.*, vol. 43, no. 2, pp. 276–284, Apr. 1996.
- [2] S. X. Chen, T. S. Low, H. Lin, and Z. J. Liu, "Design trends of spindle motors for high performance hard disk drives," *IEEE Trans. Magn.*, vol. 32, pp. 3848–3850, Sept. 1996.
- [3] S. L. Ho and W. N. Fu, "A comprehensive approach to the solution of direct-coupled multi-slice model of skewed induction motors using time stepping eddy-current finite element method," *IEEE Trans. Magn.*, vol. 33, pp. 2265–2273, May 1997.
- [4] M. Antila, E. Lantto, and A. Arkkio, "Determination of forces and linearized parameters of radial active magnetic bearings by finite element technique," *IEEE Trans. Magn.*, vol. 34, pp. 684–694, May 1998.
- [5] H. L. Li, S. L. Ho, W. N. Fu, and H. C. Wong, "Representation of star-connected stator windings in circuit-field coupled time stepping finite element model of electric machines," presented at the 9th Biennial IEEE Conf. Electromagnetic Field Computation, Milwaukee, WI, June 2000.
- [6] S. L. Ho, W. N. Fu, and H. C. Wong, "Reduction of computing time in time stepping finite element model of magnetic field computation of electric machines," presented at the 9th Biennial IEEE Conf. Electromagnetic Field Computation, Milwaukee, WI, June 2000.